Opening Windows – Increasing Window Size in Motion-Compensated ECG-gated Cardiac Vasculature Reconstruction

Chris Schwemmer, Christopher Rohkohl, Günter Lauritsch, Kerstin Müller, and Joachim Hornegger

***Abstract*—In interventional angiographic C-arm CT imaging (rotational angiography), 3-D reconstruction of coronary vasculature is a topic of ongoing research. Due to the slow gantry rotation speed, motion artefacts corrupt image quality. Many approaches use retrospective ECG-gating to limit data inconsistencies during reconstruction. This poses a trade-off between gating window size and artefact level. A large gating window reduces undersampling artefacts, but increases motion artefacts and vice versa.**

In this paper, we investigate how motion compensation can be used to successively increase the gating window size in a bootstrapping process. We use a deformable 2-D–2-D registration between the acquired projection data and a forward projection of the previous reconstruction to estimate motion inside the current gating window. We evaluated the approach using the publicly available CAVAREV platform and on six human clinical datasets. We found that an increased gating window size leads to better homogeneity and resolution of fine detailed structures and a reduction of undersampling artefacts, while motion artefacts can be controlled well up to a gating window size of 80%, depending on speed and amplitude of the motion. In addition, the use of more projection data allows for a sharper ramp filter kernel, increasing the sharpness of the reconstructed structures. The CAVAREV results showed a 10% improvement over the best result published online at the time of this writing.

I. Introduction

During coronary interventions, three-dimensional information can provide improved guidance and easier assessment, especially for complex vessel topologies. For intra-procedural imaging, an angiographic C-arm CT system is a readily available modality. But the slow rotation speed of these devices limits their temporal resolution. This leads to motion-related artefacts like motion blur and streak artefacts. A retrospectively ECG-gated reconstruction of the X-ray projection data improves temporal resolution. Only images from a specific heart phase contribute to the reconstruction. However, this presents a trade-off regarding the gating window size. Projection images within a small gating window are expected to display a similar motion state. But the small amount of data in turn leads to undersampling artefacts that strongly decrease 3-D image quality. On the other hand, a large gating window avoids undersampling artefacts, but then residual motion within the gated projection data again leads to motion artefacts.

It has been shown in previous work that motion compensation can be used to correct for residual motion in ECG-gated reconstruction [1], [2]. These approaches have in common that first, a reference image is reconstructed, that is then used for the motion estimation. Since this image needs to show as little motion-related artefacts as possible to allow for a stable motion estimation, a smaller gating window is preferred. The resulting undersampling artefacts can be reduced by using a smooth ramp filter kernel, which unfortunately also reduces spatial resolution. But still, motion estimation for projection images far from the reference heart phase (large gating window) is difficult. Therefore, in this paper, we investigate whether and how motion estimation and compensation can be used to "bootstrap" a reconstruction with a large gating window and a sharper kernel in an iterative manner.

C. Schwemmer, K. Müller and J. Hornegger are with the Pattern Recognition Lab, Department of Computer Science, and the Erlangen Graduate School in Advanced Optical Technologies (SAOT), Friedrich-Alexander-Universität Erlangen-Nürnberg, Erlangen, Germany, email: chris.schwemmer@cs.fau.de. C. Rohkohl and G. Lauritsch are with the Siemens AG, Healthcare Sector, Forchheim, Germany.

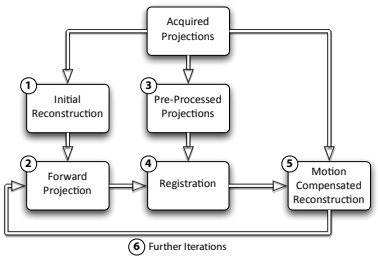

Figure 1: Illustration of our algorithm.

II. Methods

A. Motion Estimation and Compensation Algorithm

An overview of the motion estimation and compensation algorithm we used can be seen in Fig. 1. Most parts were published in [2], where a detailed description can be found. In the first step, an initial ECG-gated reconstruction is performed. In the second step, non-vascular tissue is removed by a thresholding operation. The vascular structure is forward projected using a maximum intensity forward projection. In step three, the original projection images are pre-processed using a morphological top-hat operation [1] and a thresholding, so that non-vascular tissue is also removed as much as possible. In the fourth step, the pre-processed original projections and the forward projections are registered using deformable 2-D–2-D registration in a multi-resolution scheme. In step five, a motion compensated, ECG-gated reconstruction is performed using the deformation field from the registration step. In the sixth step, the procedure is repeated for further refinement using the same or different gating parameters.

A set of parameters is available for our algorithm. All ECG-gated reconstructions are defined by the reference heart phase h_r and the size and shape of the gating window centred around

h_r. $h_r \in [0, 1]$ is expressed as a fraction of the heart cycle. The gating window is of $\cos^a$ shape [3], where $a \geq 0$ controls the edge steepness. The total size $\omega \in [0, 1]$ is given as a fraction of the heart cycle. For all gated reconstructions, streak reduction [4] was performed. Thresholding of the reconstructions before forward projection was performed by retaining only the t_r percentile of the largest voxel values. Thresholding of the original projections after top-hat filtering was performed by retaining only the t_p percentile of largest pixel values.

The current motion model is a combination of affine motion and deformable motion, where the latter is modelled by uniform cubic B-splines. We used only the affine part on the lower resolution levels and both parts on the higher levels. The B-spline model is parametrised by the number of control points c in each dimension. The cost function for registration was normalised cross-correlation and the optimisation was driven by a gradient descent method.

B. Bootstrapping Method

Since the initial reconstruction must be performed without any motion compensation, a small gating window (here: $\omega = 0.4$) is needed to avoid residual motion as much as possible. Still, remaining motion inside that window degrades image quality, which can be compensated by the algorithm described in Section II-A. A direct increase of ω in the first iteration is difficult for two reasons: Both residual motion and undersampling artefacts from the small window size limit the quality of the reference image, increasing the chance of misregistration during motion estimation. In addition, the amount of motion within the gating window increases with ω. A motion model with a larger c would then be desirable, which in turn decreases numerical stability. We therefore increase ω in an iterative fashion. For a certain ω, residual motion is compensated and the result used as a reference image for a new iteration with increased ω. Since a large number of parameter combinations is possible, we used CAVAREV to evaluate different choices and selected the best candidates for the final evaluation on clinical data.

C. Experimental Setup

1) CAVAREV*:* CAVAREV [5] is a publicly available platform for the evaluation of cardiac vasculature reconstruction algorithms. We used the cardiac motion-only dataset for our evaluation, assuming a strict breath-hold protocol. This dataset consists of 133 simulated projection images created from a software phantom that shows a thorax and contrasted left and right coronary arteries. Each projection image has a size of 960×960 pixels and an isotropic pixel size of 0.32 mm. Source-isocentre-distance was ~80 cm and source-detector-distance ~120 cm. The reconstructed 3-D volumes have an isotropic voxel size of 0.5 mm and a size of $98^3\,\mathrm{mm}^3$. The reference heart phase was selected as $h_r = 0.90$.

We created motion compensated reconstructions with 0 (initial reconstruction), 1, 2 and 3 iterations of our algorithm. Iterations 0 to 2 used $\omega = 0.4$, while in iteration 3 reconstructions with $\omega = 0.8$ and $\omega = 1.0$ were tested. In addition, each reconstruction was both done with a smooth and a normal kernel. After all experiments with 2 iterations, we selected the best scoring reconstruction for forward projection for the remaining experiments with 3 iterations.

Table I: Clinical datasets used for the evaluation. The number of projections correspond to 40%, 80% and 100% gating.

Dataset	3-D Img. Vol. [mm^3]	Heart Rate [bpm]	#Projs. Used
LCA1	$140^2 \times 101$	77 ± 0.1	53 / 106 / 133
LCA2	$152^2 \times 107$	58 ± 0.4	53 / 105 / 133
LCA3	$152^2 \times 114$	52 ± 0.7	54 / 106 / 133
RCA1	$152^2 \times 110$	68 ± 1.5	53 / 105 / 133
RCA2	$131^2 \times 109$	71 ± 2.1	53 / 105 / 133
RCA3	$143^2 \times 119$	54 ± 1.9	54 / 107 / 133

Table II: Motion model configuration for the experiments.

	Resolution Level		
	Low	Med	High
1. & 2. Iter.	affine	affine	+B-spline, $c = 6$
3. Iter.	affine	+B-spline, $c = 6$	+B-spline, $c = 12$

2) Human Clinical Datasets: Six human clinical datasets were used for the evaluation (cf. Table I): In LCA1, LCA2 and LCA3, a left coronary artery was imaged. The patient in dataset LCA2 had a total occlusion in the proximal part of the LAD, which means that no contrast agent reached the LAD beyond this point. In RCA1, RCA2 and RCA3, a right coronary artery was imaged. All datasets were acquired using a five second rotational angiography with selective contrast agent administration (1–2 ml/s) on an Artis zeego C-arm device (Siemens AG, Healthcare Sector, Forchheim, Germany). Source-isocentre-distance was ~80 cm and source-detector-distance ~120 cm. Each dataset consists of 133 projection images with a size of 1240×960 pixels and an isotropic pixel size of 0.308 mm. The reconstructed 3-D volumes have an isotropic voxel size of 0.5 mm. The reference heart phase was selected as $h_r = 0.75$ for all human datasets.

Again, we created motion compensated reconstructions with 0, 1, 2 and 3 iterations. A smooth kernel was used for iterations 0 to 2 and both kernels were tested for iteration 3, due to the results of the CAVAREV evaluation (cf. Section III-A). As in the CAVAREV experiments, a 40% gating window was used for iterations 0 to 2 and both 80% and 100% for iteration 3.

3) Common Parameters: Thresholding was performed at $t_r = 0.005$ and $t_p = 0.2$. The size of the morphological kernel for top-hat filtering was 3.85 mm. We employed a multi-resolution registration scheme with 3 levels. The motion model configuration for the different experiments is listed in Table II. The maximum number of optimisation steps on each level was set to 200 for the affine and 250 for the deformable registration. Optimisation was stopped if the gradient magnitude of the NCC was below $3 \cdot 10^{-4}$. For $\omega = 0.4$ and $\omega = 0.8$, a $\cos^4$ window was used, i.e. $a = 4$. For ungated reconstructions ($\omega = 1.0$), $a = 0$ was used. Streak reduction was used for $\omega = 0.4$ and $\omega = 0.8$.

D. Evaluation

Qualitative evaluation was carried out visually. The quantitative evaluation of the CAVAREV experiments was done using the metric $Q_{3\mathrm{D}} \in [0, 1]$ provided by the platform [5], which describes the morphological similarity of a reconstruction to the ground truth data. $Q_{3D} = 1$ would indicate the best possible value.

Table III: CAVAREV results. The percentage is the size of the gating window ω.

	Q_{3D}
Initial, smooth kernel	0.744
Initial, normal kernel	0.739
1 Iter., 40%, smooth kernel	0.776
1 Iter., 40%, normal kernel	0.771
2 Iter., 40%, smooth kernel	0.776
2 Iter., 40%, normal kernel	0.773
3 Iter., 80%, smooth kernel	0.808
3 Iter., 80%, normal kernel	0.810
3 Iter, 100%, smooth kernel	0.805
3 Iter, 100%, normal kernel	0.821

For the quantitative evaluation of the human clinical datasets, we calculated the vessel sharpness [6] of continuous vessel segments along each reconstructed tree. We selected the same branch along the LAD and LCX of each left coronary dataset, and the main branch of each right coronary artery dataset. The average lengths of the selected branches were 198 mm (LAD for LCA1 and LCA3), 174 mm (LCX) and 183 mm (RCA). The LAD of dataset LCA2 could only be segmented for the first 79 mm due to the occlusion. Along each branch, sharpness measurements were taken with a spacing of 1 mm and the reported values are the average values of all measurements for that branch.

III. Results and Discussion

A. CAVAREV *Experiments and Parameter Selection*

Table III lists the Q_{3D} values for the CAVAREV experiments ($Q_{3D} = 0.744$ is the best value published online at the time of this writing). For this dataset, a second iteration with $\omega = 0.4$ and a smooth kernel does not change the result measurably. In addition, it can be seen that a smooth kernel leads to slightly better Q_{3D} values. From a theoretical viewpoint, $\omega = 0.4$ results in a low number of projections used for reconstruction, promoting undersampling artefacts. These are amplified by a sharper kernel. Therefore, we suggest a more conservative smooth kernel for both the initial and all motion compensated reconstructions that use a 40% gating window size. If a larger gating window is used, an improved reconstruction of the vasculature can be obtained, as shown by the higher Q_{3D} scores. Additionally, a sharper kernel does improve the achievable quality, since undersampling artefacts are not as dominant anymore.

Volume renderings of the reconstructions of selected parameter combinations can be seen in Fig. 2. Comparing Fig. 2b ($\omega = 0.4$) and 2c ($\omega = 0.8$), a clear decrease in artefact level can be observed as indicated by the arrows. In addition, vessel structures appear more homogeneous with a better visibility of distal parts. While an ungated reconstruction further improves vessel homogeneity, motion blur and an increase in artefact level can be observed in Fig. 2d.

B. *Human Clinical Datasets*

Table IV shows the vessel sharpness values for all datasets and reconstructions. Over all datasets, vessel sharpness decreased when going from a 40% to an 80% or 100%

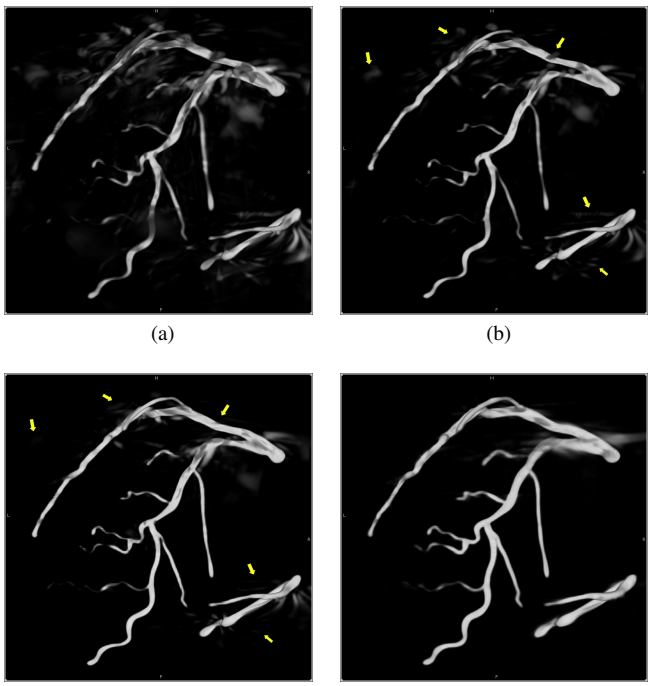

(a) (b) (c) (d)

Figure 2: Reconstruction results of the CAVAREV dataset. (a) Initial reconstruction. (b) 2 iter., 40%, smooth kernel. (c) 3 iter., 80%, normal kernel. (d) 3 iter., 100%, normal kernel. The grey scale window was 1000 HU.

Table IV: Average vessel sharpness in 1/mm. The percentage is the size of the gating window ω, s.k. denotes smooth and n.k. normal kernel.

(a) Left coronary arteries.

	LCA1		LCA2		LCA3	
	LAD	LCX	LAD	LCX	LAD	LCX
Initial	0.410	0.368	0.324	0.354	0.453	0.423
1 Iter., 40%, s.k.	0.482	0.446	0.443	0.479	0.512	0.511
2 Iter., 40%, s.k.	0.486	0.464	0.451	0.484	0.524	0.516
3 Iter., 80%, s.k.	0.457	0.441	0.355	0.400	0.497	0.495
3 Iter., 80%, n.k.	0.550	0.523	0.498	0.543	0.633	0.589
3 Iter, 100%, s.k.	0.387	0.387	0.367	0.409	0.429	0.481
3 Iter, 100%, n.k.	0.451	0.456	0.467	0.528	0.537	0.555

(b) Right coronary arteries.

	RCA1	RCA2	RCA3
Initial	0.358	0.375	0.447
1 Iter., 40%, s.k.	0.500	0.457	0.483
2 Iter., 40%, s.k.	0.515	0.460	0.484
3 Iter., 80%, s.k.	0.481	0.436	0.451
3 Iter., 80%, n.k.	0.546	0.509	0.535
3 Iter, 100%, s.k.	0.451	0.410	0.427
3 Iter, 100%, n.k.	0.513	0.475	0.491

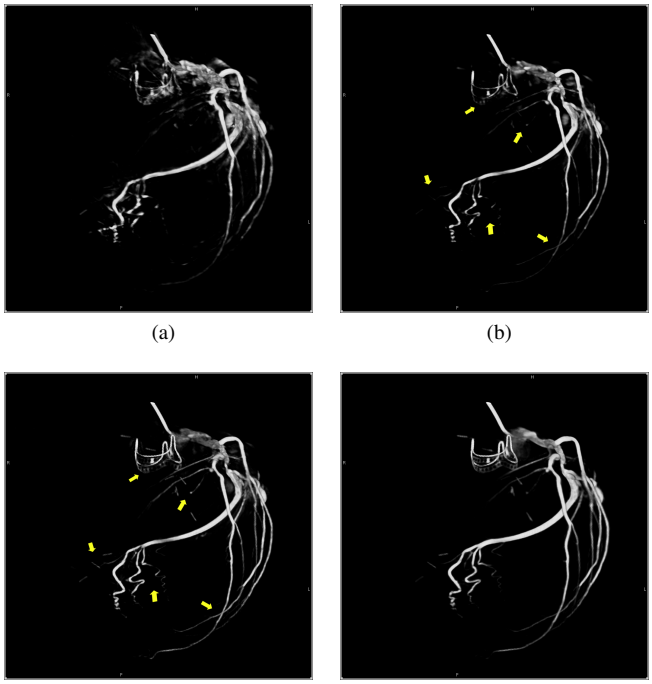

(a) (b) (c) (d)

Figure 3: Reconstruction results of dataset LCA3 (left anterior oblique view). (a) Initial reconstruction. (b) 2 iter., 40%, smooth kernel. (c) 3 iter., 80%, normal kernel. (d) 3 iter., 100%, normal kernel. The grey scale window was 1000 HU.

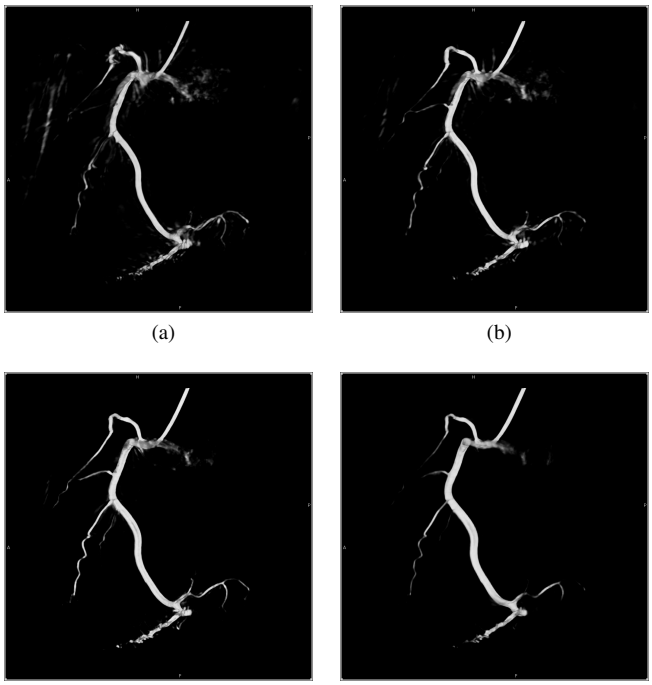

(a) (b) (c) (d)

Figure 4: Reconstruction results of dataset RCA3 (left sagittal view). (a) Initial reconstruction. (b) 2 iter., 40%, smooth kernel. (c) 3 iter., 80%, normal kernel. (d) 3 iter., 100%, normal kernel. The grey scale window was 1000 HU.

gating window and a smooth kernel. But this effect can be compensated by switching to a sharper kernel: The best sharpness results for all datasets were achieved with $\omega = 0.8$ and a normal kernel.

In Fig. 3 and 4, reconstruction results for two datasets are shown as volume renderings. Fig. 3 illustrates the benefits of increasing the gating window size and being able to use a sharper kernel: Vessel homogeneity is greatly increased (cf. arrows), which in turn increases the visible length of small distal vessels. In addition, the depiction of the artificial valve is improved both in Fig. 3c and even more in Fig. 3d. While the same observations about vessel homogeneity and visibility hold for Fig. 4c, Fig. 4d shows that $\omega = 1.0$ did not improve but decrease vessel visibility for dataset RCA3 compared to $\omega = 0.8$. Again, we attribute this to not fully compensated motion.

IV. Conclusion

Gating window size in ECG-gated cardiac reconstruction is a trade-off between undersampling and motion-related artefacts. The latter can be reduced by residual motion compensation. But motion estimation and compensation becomes more difficult with large window sizes. We investigated how this can be overcome by an iterative process that successively increases the window size (bootstrapping). We found that motion-related artefacts can be controlled well up to a window size of 80%. The larger window reduces undersampling artefacts and leads to better homogeneity and resolution of fine detailed structures. In addition, more usable projection data allows for a sharper ramp-like filter kernel, which in turn increases sharpness and resolution of the reconstructions.

Acknowledgement

The authors gratefully acknowledge funding of the Erlangen Graduate School in Advanced Optical Technologies (SAOT) by the German Research Foundation (DFG) in the framework of the German excellence initiative. The authors also would like to thank Prof. Dr. D. Böcker and Dr. P. Skurzewski, St. Marienhospital Hamm, Germany for acquiring clinical data.

Disclaimer: The concepts and information presented in this paper are based on research and are not commercially available.

References

[1] E. Hansis, D. Schäfer, O. Dössel, and M. Grass, "Projection-based motion compensation for gated coronary artery reconstruction from rotational x-ray angiograms," *Phys. Med. Biol.*, vol. 53, no. 14, pp. 3807–3820, 2008.

[2] C. Schwemmer, C. Rohkohl, G. Lauritsch, K. Müller, and J. Hornegger, "Residual Motion Compensation in ECG-Gated Cardiac Vasculature Reconstruction," in *Proc. 2nd Intl. Mtg. on image formation in X-ray CT*, F. Noo, Ed., Salt Lake City, UT, USA, June 2012, pp. 259–262.

[3] D. Schäfer, J. Borgert, V. Rasche, and M. Grass, "Motion-compensated and gated cone beam filtered back-projection for 3-D rotational X-ray angiography," *IEEE Trans. Med. Imaging*, vol. 25, no. 7, pp. 898–906, Jul. 2006.

[4] C. Rohkohl, G. Lauritsch, A. Nöttling, M. Prümmer, and J. Hornegger, "C-Arm CT: Reconstruction of Dynamic High Contrast Objects Applied to the Coronary Sinus," in *IEEE NSS/MIC Record*, Dresden, Germany, Oct. 2008, pp. M10–328.

[5] C. Rohkohl, G. Lauritsch, A. Keil, and J. Hornegger, "CAVAREV – An Open Platform for Evaluating 3D and 4D Cardiac Vasculature Reconstruction," *Phys. Med. Biol.*, vol. 55, no. 10, pp. 2905–2915, 2010.

[6] D. Li, J. Carr, S. Shea, J. Zheng, V. Deshpande, P. Wielopolski, and J. Finn, "Coronary Arteries: Magnetization-prepared Contrast-enhanced Threedimensional Volume-targeted Breath-hold MR Angiography," *Radiology*, vol. 219, no. 1, pp. 270–277, April 2001.